Mode Partition Noise and Chaos: An Experimental Exploration in a Multimode Microchip Nd:YVO_4 Solid-State Laser

Jyh-Long Chern[1], Siao-Lung Hwong[1], A-Chuan Hsu[1], and Kenju Otsuka[2]
[1]*Department of Physics, National Cheng Kung University, Tainan 701, Taiwan*
[2]*Department of Applied Physics, Takai University 1117, Kitakaname, Hiratsuka, Kanagawa 259-12, Japan*
(Received January 28, 2002)

Based on a singular-value-decomposition method, we used the time series of a multimode Nd:YVO_4 microchip solid state laser to explore the interplay between mode-partition noise and chaos. We experimentally show that, as chaos occurs, the noise level that of the modal output can be smaller than of the total output. In contrast, in the case of a relaxation oscillation, the common feature of mode partition noise persists, i.e., total output noise is smaller.

PACS. 42.60.Mi – Dynamical laser instabilities; noisy laser behavior.
PACS. 05.45.+b – Theory and models of chaotic systems.

With a reflective grating, lasing modes can be partitioned and the noise levels of modal outputs will be enhanced such that the modal output noise is larger than that of the total output. This generic feature of laser systems is named *mode partition noise* [1]. In laser physics, intensity fluctuations are usually characterized by relative intensity noise (RIN) [2] defined as

$$RIN \equiv \frac{<\delta P^2>}{<P>^2} = \frac{<(P-<P>)^2>}{<P>^2}, \tag{1}$$

where P is the measured power and $<P>$ is its time average. The RIN can be extended to the frequency domain so that mode partition noise also can be characterized [2]. Nevertheless, it can be recognized in the early literature that the spectral RIN becomes larger as the measured frequency interval is close to the relaxation oscillation [3]. Under this condition, the RIN of the total output can be larger than that of the modal output, while outside the frequency region of the relaxation oscillation the feature of mode partition noise persists. This peculiar feature is intriguing in terms of nonlinear dynamics, because in nonlinear systems the spectrum of chaos is broad-band in which there are embedded many "relaxation-oscillation-like" frequencies. Hence, a crucial question is *the persistence of mode partition noise in chaos*. Unfortunately, common RIN could not provide us with a conclusive answer to the above question. To illustrate this point, let us suppose that a signal P_S is with a noise P_N such that the detected power $P = P_S + P_N$. By definition,

$$RIN = \frac{<P_S^2> - <P_S>^2 + D}{<P_S>^2} = RIN_S + \frac{D}{<P_S>^2}, \tag{2}$$

where for simplicity, we assume $< P_N >= 0$ and $< P_N(t)P_N(t') >= D\delta(t-t')$ in which D denotes the noise strength. Meanwhile, we also assume the correlation $< P_N P_S >= 0$ and denote the RIN of P_S as RIN_S. Because $RIN_S = 0$ can only be true for a constant-value signal, the RIN could not be used to discriminate the noise level of non-steady signals. Even though an improvement for periodic signals can be established in the spectral domain, the spectral RIN is still ambiguous for chaotic signals, due to the broadened-band characteristics inherent in chaos. Thus, to solve the problem it is necessary to develop a different characterization, such that noise and chaos can be simultaneously recognized. This is a difficult issue, but it is not impossible to achieve by a geometrical means [4]. The basic idea of Ref. [4] is that the dimension of a chaotic attractor is small, while in contrast, noise is infinite-dimensional. With a phase space reconstruction of the time series one measured the noise will dominate the redundant dimensions by which the noise level can be distinguished. The purpose of this paper is to explore the persistence of mode partition noise in chaos based on this geometrical scheme. It will be experimentally shown that *as chaos occurs, the noise level of the modal output can be smaller than that of the total output*, which shows a violation of the common understanding of mode-partition noise. In contrast, in the case of relaxation oscillation, the common feature of mode partition noise persists, i.e., total output noise is smaller.

Practically, as laser power is measured in a high-speed data flow, the ac part is picked up at one port. Hereafter, we only consider the dc-removed power in our analysis, for this, we can have a time series $P(k\Delta)$ where Δ is the time difference between two successive samplings and $k = 1, 2, ..., (N+d-1)$. Here, d is the embedding dimension for phase space reconstruction and $(N+d-1)$ is the total number of data. We can construct a d-dimensional vector $Y(t) = [P(t), P(t+\Delta), ..., P(t+(d-1)\Delta)]$. With these vectors, one can define a trajectory matrix A

$$A = \begin{bmatrix} P(t) & P(t+\Delta) & \cdots & P(t+(d-1)\Delta) \\ P(t+\Delta) & P(t+2\Delta) & \cdots & P(t+d\Delta) \\ \vdots & \vdots & \ddots & \vdots \\ P(t+(N-1)\Delta) & P(t+N\Delta) & \cdots & P(t+(N+d-1)\Delta) \end{bmatrix}, \tag{3}$$

which contains all dynamical information [4]. Using the SVD method, the matrix A can be decomposed such that $A = VSU^T$, where V is an $N \times d$ orthogonal matrix, U is a $d \times d$ orthogonal matrix and S is a $d \times d$ diagonal matrix, i.e., $(V^TV)I_{i,j} = \delta_{i,j}$, $(U^TU)I_{i,j} = (UU^T)I_{i,j} = \delta_{i,j}$, $S_{i,j} = \delta_{i,j}s(i)$ where the index i and $j = 1, 2, \ldots, d$. The matrix S is the singular-value matrix of A and $s(i)$ is the corresponding singular value at the i-th index. Since $U^T(A^TA)U = S^2$ and $(A^TA)U = S^2U$, $s(i)^2$ are eigenvalues of A^TA and U is the corresponding set of eigenvectors. We normalized these $s(i)^2$ with their total sum and rearranged them in descending order [4]. The rearranged and normalized $s(i)^2$ versus the index i is the SVD eigenvalue spectrum. This SVD spectrum is our basic tool to explore the interplay between mode partition noise and chaos.

Our analysis is essentially based on our previous work on the SVD spectrum [4]. We summarize the main results here.

(1) For the chaotic signal, the SVD eigenvalue spectrum displays two segments when the dimension d is large enough. The first segment presents a quickly decaying part (exponential decay), which can be used to identify the signature of chaos. The second segment is a slowly decaying part that is approximately horizontal. This horizontal level can be used to identify the noise level which is named the "noise floor".

(2) On the other hand, for periodic and quasi-periodic signals the first segment will be replaced by a sudden dropping.
(3) Furthermore, as noise strength is increased, the floor will be lifted while the first segment remains unchanged. In practice, the magnitude of eigenvalues for the slowly decaying part can be approximately averaged. This averaged value is denoted as f, which indicates the strength of the noise embedded in the time series.
(4) The strength ratio between the noise I_N and the "signal without the noise" I_S follows

$$R = \frac{I_N}{I_S} \cong \sqrt{f} \times 10. \tag{4}$$

Here, the factor 10 originats from the power law relation between the strength of noise and the SVD noise floor. Equation (4) has been numerically verified in a variety of dynamical systems [4]. In our analysis, we set the embedding dimension d = 100. We also label the noise floors of total output and modal output as f_t and f_m respectively.

Next, we describe our experimental setup. The schematic diagram is shown in Fig. 1. Our system is a free-running laser diode (LD)-pumped microchip Nd:YVO_4 laser. LD and Nd:YVO_4 (1 mm thick, 1% Nd^{3+}-doped, and output coupling 5±2% at 1064 nm) lasers are available from CASIX, Inc. The laser crystal (Nd:YVO_4) is inserted into a 2 mm-thick copper mount and the temperature is controlled at 25°C by a temperature controller (ILX, LDT-5910B). The pumping beam (with wavelength at λ_p = 808 nm) from the LD, which is also temperature-controlled, is focused onto the laser crystal with a GRIN lens (0.22 pitch). We also use a noise filter to eliminate the pumping noise caused by the LD current driver (ILX, LDC-3744) and an interference filter (60% transmission at 1064 nm and zero-transmission for the rest) to reduce the influence of the pumping light on detection. We expect that noisy power fluctuations should be small. A multi-wavelength meter (HP 86120B) is employed to monitor the variation of each lasing mode, and possible fiber-feedback induced instability has been avoided. We utilize two low-noise detectors (New Focus 1611, bandwidth 1 GHz) for detection. To partition the lasing modes, we use a reflective grating which has 1200 g/mm and is blazed at 1000 nm. For measurement, an oscilloscope with 1.5 GHz bandwidth (HP 54845A) is used. On the other hand, data acquisition is done after transience, to avoid any possible misleading results in the SVD analysis. In time-series data acquisition, we also have used an N.D. filter to reduce the power of the total output such that the two measured powers (total output and modal output) are roughly equal, and the sampling rate of data acquisition is 500 MHz.

The input-output characteristic (common P-I curve) is shown in Fig. 2. A π-polarized TEM_{00} mode was observed in the entire pumping domain. As pumping power is increased, the total number of modes changes from one to two, and then three modes. The symbol 2(3) means that there are totally three modes totally in which one of the modes is very small and its value remains almost the same, while for the rest of the two modes, their output powers increase with the pumping. The wavelength of this "clamped mode" is 1064.449 nm and its power is around 0.03 mW. The total number of modes in different pumping regions provides a simple classification of laser dynamics.

Typical time series of the total and modal outputs are noisy as shown in Fig. 3 (a) and (b). Referring to Fig. 3(c), both SVD eigenvalue spectra do show sudden drops with different noise floors. The sudden drops indicate that both the total and modal outputs are simply relaxation oscillations driven by noise. On the other hand, the noise floor is slightly inclined which means

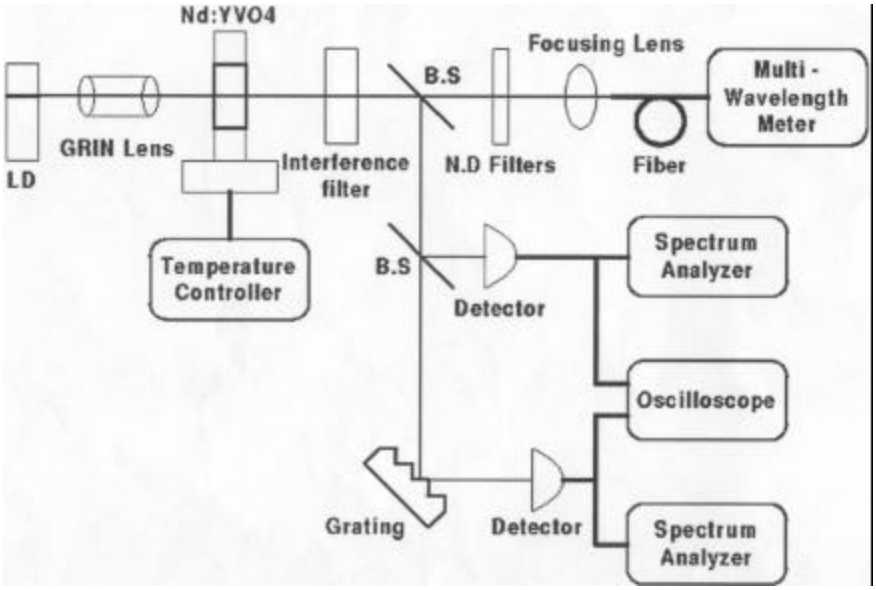

FIG. 1. The experimental setup of a diode-pumped microchip Nd:YVO_4 laser.

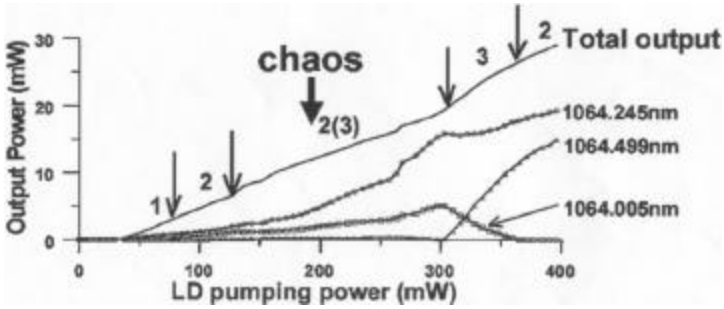

FIG. 2. The input-output characteristics where the corresponding wavelengths are labeled on the right-hand side. The digital number shown above the curve is the total number of modes, while 2(3) is used to denote a chaotic region in which two of the modes are large but one mode is very small.

it is a dynamical noise [4]. To estimate the noise level of an inclined floor, we take a line fitting to determine the intersection between the first segment and the noise floor. This intersection is the starting dimension for averaging the eigenvalues of the noise floor. As shown by Fig. 3(c), the noise floor of the total output f_t is smaller than that of the modal outputs f_m. In this case, the corresponding strength ratio of the total output R_t is also smaller than that of the modal output R_m. This can be recognized as the appearance of the common feature of mode partition noise. These typical features occur in the regions, 1, 2, and 3, but not in the region 2(3) of Fig. 2.

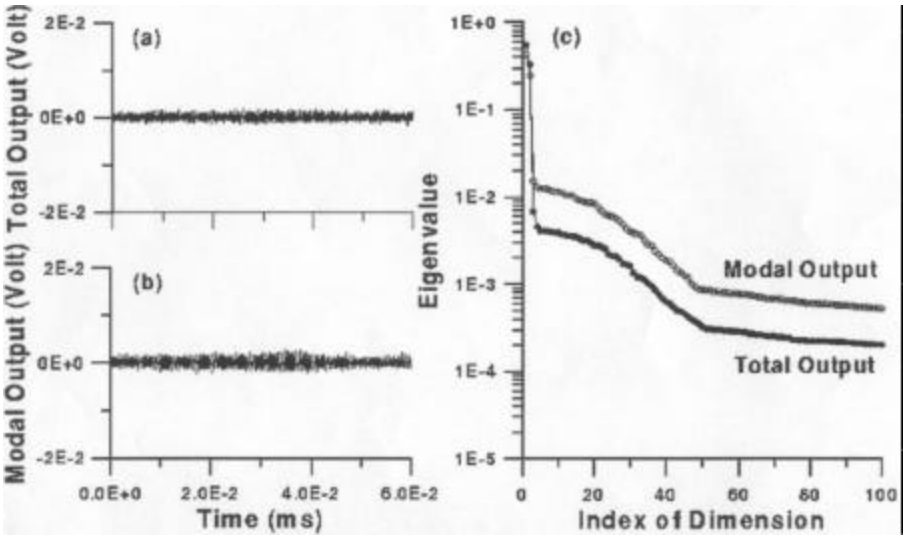

FIG. 3. Typical dynamical characteristics for the regions labeled 1, 2, and 3 in Fig. 2(a) total output time series, (b) modal output time series, and (c) their corresponding SVD eigenvalue spectra where the total output case is denoted by a solid circle while the empty one indicates the modal output. Here the pumping power is 78 mW.

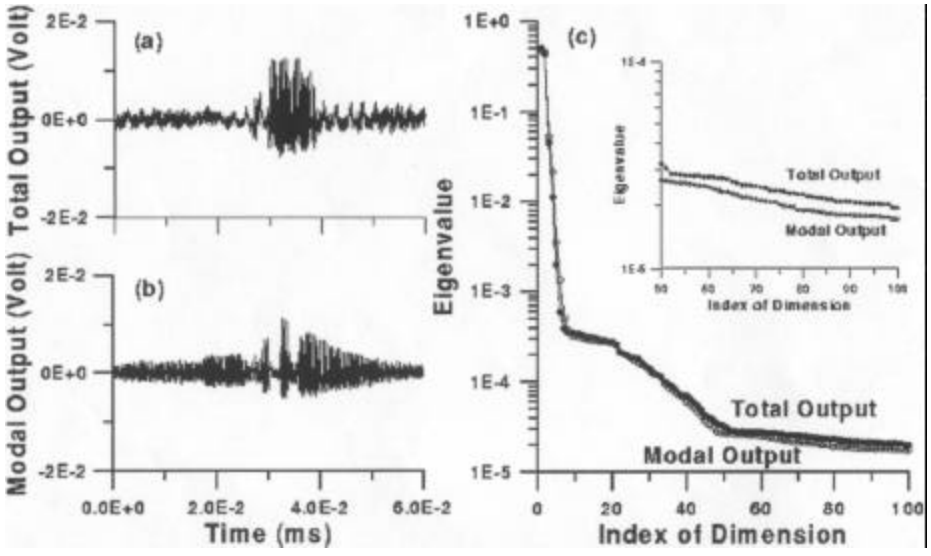

FIG. 4. Typical dynamical characteristics for the region labeled 2(3) in Fig. 2. (a) total output time series, (b) modal output, time series, and (c) the SVD eigenvalue spectra in which the solid circle is for total output and the empty one is for the modal output. An enlarged portion is used to show the reversing of the noise floor. Here the pumping power is 137 mW.

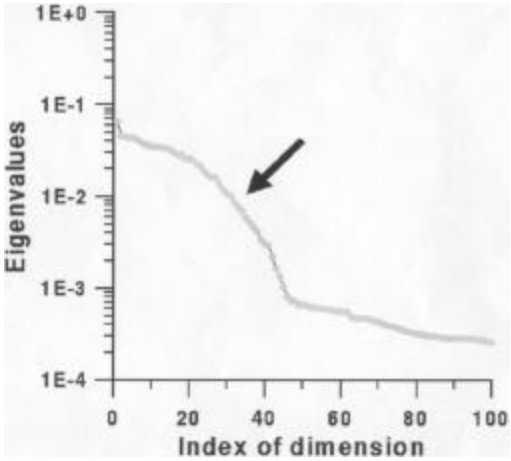

FIG. 5. Typical SVD eigenvalue spectrum of the channel noise of the oscilloscope used in the experiment. A hump indicated by an arrow can be seen in the noise floor.

In contrast, for the region 2(3) of Fig. 2, the time series fluctuates extensively and intermittently, as partially shown in Fig. 4(a) and (b). It exhibits wild "random" bursts in the whole period of time. The SVD signature is shown in Fig. 4 (c) and, remarkably, the SVD eigenvalue spectrum of total output shows an exponential decay, which is a signature of chaos. In the mean time, the noise floors of f_t and f_m have been reversed. Now, it is $f_t > f_m$ ($R_t > R_m$). Intensive evaluations of SVD eigenvalue spectra over the whole pumping region have been done and the features reported above remain. The occurrence of an intermittent chaotic burst is crucial. Its origin has yet to be known, however, the appearance of a clamped mode is considered to be the cause of instability. It should be emphasized that the common feature of mode partition noise, i.e., modal output noise is larger than total output noise, can be identified only in the absence of chaos. Indeed, the signature of chaos (exponential decay in the SVD spectrum) does not appear in the regions labeled as 1, 2 and 3 in Fig. 2. In these regions, both the total output and the modal output exhibit essentially noise-driven relaxation oscillations. In contrast, as chaos appears, total output noise increased and its noise level is larger than that of the modal output. This unusual feature persists in a wide pumping range, the region 2(3) in Fig. 2, suggesting a unique interplay between noise and chaos.

There is some difference between the experimental results and the previous numerical simulation shown in Ref. 4. In the experiment, there is one more hump in the noise floor. To identify the origin of the noise hump, we blocked out the light beam, disconnected the detector and then picked up the time series for the SVD analysis. The result is shown in Fig. 5 where a similar hump can be seen. Hence, this hump is due to the channel noise caused by the oscilloscope. Nevertheless, the noise levels of signals are still significant enough and can be identified as shown by Fig. 2 and 3. Indeed, detector noise and the channel noise of the oscilloscope could be different for different detectors and channels. To remove the ambiguity caused by simultaneous measurement where two detectors and two channels have to be employed, we take a statistical approach for double-checking. We use the same detector and the same channel of the oscilloscope in the measurements of the total output and the modal output. The measurements are taken

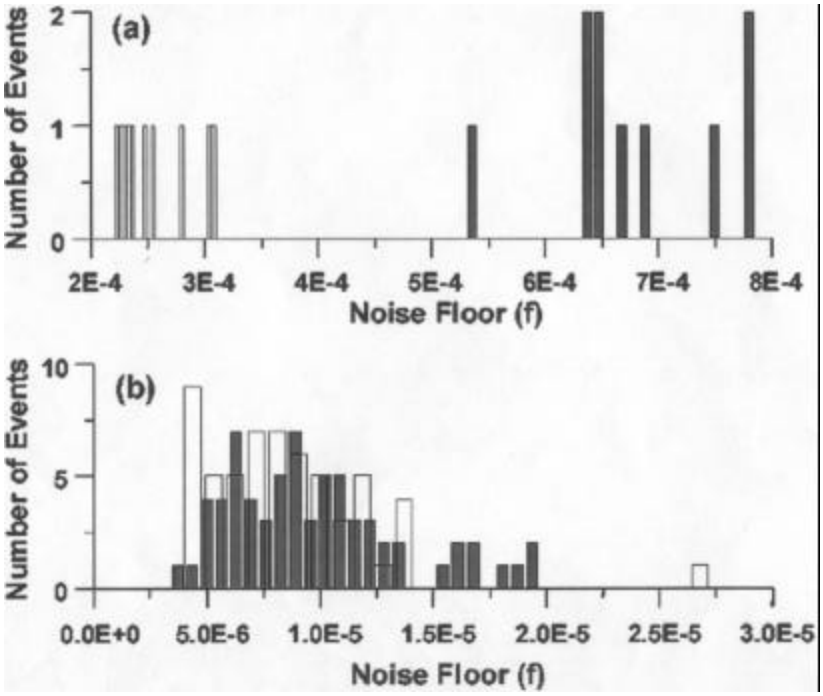

FIG. 6. Statistical distributions of the noise floors for the total output ft and the modal output, fm, where (a) is for the relaxation oscillation case and (b) chaos. The empty column denotes f_t while the solid one is for f_m.

repeatedly many times. Thus, the result of the comparison is not simultaneous, but statistical. As shown by Fig. 6(a), which is for the relaxation oscillation case, the noise floor of the model output is larger than that of the total output. This shows that statistically the characteristics of mode partition noise persist. But in the case of chaos, the two distributions have become close and overlapping as shown by Fig. 6(b). The noise level of the total output does have many chances to become larger than that of the modal output. This supports our previous simultaneous measurement.

In conclusion, our experimental results suggest that as chaos occurs, the total output noise can be larger than the modal output noise. This may imply the occurrence of a violation of mode partition noise. However, it should be admitted that Eq. (4) should fail in the cases of strongly "correlated noise" (dynamical noise). Only in the cases of weakly correlated noise, can the result of Eq. (4) be approximately correct, as shown by Ref. 4. Hence, Eq. (4) allows for measuring only a part of the noise, although it may be appropriate enough for the present study due to the small dynamical noise inherent in the laser system. It is true that the analysis of dynamical noise with chaos remains a difficult topic of current interest [5]. Our work does suggest that a further reconsideration of mode partition noise should be worthwhile. Meanwhile, there is one concern about the origin of the noise here. In some cases, pumping noise is essential [6]. However, the violation is only found in the 2(3) region. In contrast, a higher pumping (or a lower pumping) does present the common feature of mode partition noise. Thus, it seems that the influence of

pumping noise is not so essential in considering the interplay between mode partition noise and chaos here.

Acknowledgement

This work is partially supported by the National Science Council, Taiwan, ROC under contract number: NSC88-2112-M-006-001.

References

[1] See P.-L. Liu in Coherence, Amplification, and Quantum Effects in Semiconductor Lasers, ed. by Y. Yamamoto, (John Wiley & Sons, New York, 1991) and reference therein.
[2] K. Petermannn, Laser Diode Modulation and Noise, (Kluwer, Tokyo, 1991).
[3] H. Jackel, "Lichtemissionsrauschen und dynamisches Verhalten von GaAlAs-Heterosctruktur-Diodenlasern im Frquenzbereich 10 NHz bis 8 GHz," (Dissertation ETH Zurich No. 6447, Zurich, Switzerland, 1980); also see p. 165 of Ref. [2].
[4] J.-S. Lih, J.-Y. Ko, J.-L. Chern, and I.-M. Jiang, Europhysics Lett. **40**, 7 (1997); J-Y. Ko, J.-S. Lih, M.-C. Ho, C.-C. Tsai, and J.-L. Chern, Chin. J. Physics **37**, 449 (1999).
[5] Coping with Chaos, ed. by E. Ott, T. Sauer and J. A. Yorke, (Wiley, New York, 1994).
[6] R. Roy, A. W. Yu, and S. Zhu, Phys. Rev. Lett. **55**, 2794 (1985).